C. R. Physique 12 (2011) 921–927

Contents lists available at SciVerse ScienceDirect

Comptes Rendus Physique

www.sciencedirect.com

Prix Georges Charpak 2011

Study of CP violation at the LHCb experiment at CERN

Étude de la violation de CP avec l'expérience LHCb au CERN

Patrick Robbe

LAL, Université Paris-Sud, CNRS/IN2P3, 91898 Orsay cedex, France

ARTICLE INFO

Article history:
Received 13 October 2011
Accepted 26 October 2011
Available online 17 November 2011

Presented by Jacques Villain

Keywords:
Particle physics
CP violation
LHC

Mots-clés :
Physique des particules
Violation de CP
LHC

ABSTRACT

The LHCb experiment is a particle detector located at the LHC and dedicated to b and c quark studies, in particular, the study of CP violation. The concept and the performance of the detector will be presented, together with first results of the experiment. The recorded integrated luminosity of 0.3 fb^{-1} has allowed LHCb to obtain already significant important measurements concerning tests of the presence of New Physics effects in the decay of B_s mesons.

RÉSUMÉ

L'expérience LHCb est un détecteur de particules situé auprès du LHC et qui est dédié à l'étude des quarks b et c. Le concept et les performances du détecteur seront présentés ainsi que des premiers résultats obtenus. La luminosité intégrée de 0.3 fb^{-1} enregistrée a déjà permis à LHCb d'obtenir des résultats importants concernant d'éventuels signes de Nouvelle Physique dans les désintégrations des mésons B_s.

1. Introduction

LHCb is an experiment dedicated to the study of b and c quark physics and located at the Large Hadron Collider (LHC) at the European Centre for Particle Physics (CERN) in Geneva, Switzerland. The goal of the experiment is to check whether the Standard Model (SM) is able to describe rare decays of beauty and charm-flavoured hadrons, or whether an extension is necessary, hereafter called "New Physics" (NP). New Physics could, for example, appear in the B_s^0 mixing phase, measured with $B_s^0 \to J/\psi\phi$ decays.[1] The purpose of the experiment is to improve the precision of the existing measurements to achieve the necessary sensitivity to NP effects. LHCb will also extend the current knowledge of b quarks by studying the properties of heavy b-hadrons, like B_s^0, Λ_b or B_c^+, which are produced in large quantities by the LHC collisions, and thanks to a detector optimised for b-physics.

2. CP violation

Particle physics aims at studying the fundamental constituents of matter, how they interact together and how they decay. Fig. 1 shows the elementary particles, divided into three groups: leptons, quarks and force carrier bosons. Leptons

E-mail address: robbe@lal.in2p3.fr.

[1] If not explicitly written, corresponding anti-particle decays are also implied.

1631-0705/$ – see front matter
doi:10.1016/j.crhy.2011.10.019

FERMIONS *matter constituents*
spin = 1/2, 3/2, 5/2, ...

Leptons		*spin = 1/2*
Flavour	Mass (GeV/c^2)	Electric charge
ν_L *(lightest neutrino)*	(0-0.13)x10^{-9}	0
e *(electron)*	0.000511	-1
ν_M *(middle neutrino)*	(0.009-0.13)x10^{-9}	0
μ *(muon)*	0.106	-1
ν_H *(heaviest neutrino)*	(0.04-0.14)x10^{-9}	0
τ *(tau)*	1.777	-1

Quarks		*spin = 1/2*
Flavour	Approx. Mass (GeV/c^2)	Electric charge
u *(up)*	0.002	2/3
d *(down)*	0.005	-1/3
c *(charm)*	1.3	2/3
s *(strange)*	0.1	-1/3
t *(top)*	173	2/3
b *(bottom)*	4.2	-1/3

BOSONS *force carriers*
spin = 0, 1, 2, ...

Unified Electroweak		*spin = 1*
Name	Mass (GeV/c^2)	Electric charge
γ *(photon)*	0	0
W$^-$	80.39	-1
W$^+$	80.39	1
Z^0	91.188	0

Strong (color)		*spin = 1*
Name	Mass (GeV/c^2)	Electric charge
g *(gluon)*	0	0

Fig. 1. Tables of elementary particles.

and quarks are divided into three flavour families; the lightest one (u, d, e and ν_e) is the family of which is made the matter surrounding us. The LHCb experiment is studying heavy quarks: c (charm) and b (beauty). Mesons discussed in this article are bound states of one quark and one anti-quark: $B^0 = \bar{b}d$, $B^+ = \bar{b}u$, $B_s^0 = \bar{b}s$, $J/\psi = c\bar{c}$, $\phi = s\bar{s}$ and $K^+ = \bar{s}u$.

The theoretical framework describing particle physics is the Standard Model (SM). It is a model accounting successfully for a large number of parameters concerning, in particular, electromagnetic and weak interactions. However, it fails to explain several aspects of particle physics, including the asymmetry between matter and anti-matter. For each particle of matter (P), there exists the corresponding anti-particle of anti-matter ($\bar{P}$). The existence of anti-matter was first predicted in 1928 by P. Dirac [1] and the first observation of a positron (anti-electron) made by C. Anderson in 1933 [2].

The surrounding universe is composed only of matter, and not of anti-matter. One possibility to explain this large asymmetry would be that anti-matter is located in far areas of the universe. No experimental evidence of this has been observed so far, but ongoing experiments are still looking for sources of anti-matter in the universe, such as the AMS experiment [3], installed in the International Space Station in May 2011. The second possibility is that the anti-matter disappeared quickly after the big-bang by annihilation with the matter, when the universe was created. A. Sakharov postulated that one condition for this to happen is the existence of "CP violation" [4].

The CP transformation is the product of the two discrete symmetry operators:

- C, charge conjugation, which transforms a particle into its anti-particle, $P \to \bar{P}$;
- P, parity, which reverts the spatial components, $\vec{x} \to -\vec{x}$.

CP violation means that the CP operator is not an exact symmetry and that matter and anti-matter have different behaviour in their interactions.

Within the Standard Model, CP violation can appear in strong interactions and in weak interactions. CP violation in strong interactions has been measured to be extremely small. The research conducted at the LHCb experiment is looking at CP violation in weak interactions. Quarks indicated in Fig. 1 are not eigenstates of the weak interaction, so under a weak interaction process, a quark can change flavour. The probability to change flavour is given by the Cabibbo–Kobayashi–Maskawa (CKM) matrix [5]:

$$V_{\mathrm{CKM}} = \begin{pmatrix} V_{ud} & V_{us} & V_{ub} \\ V_{cd} & V_{cs} & V_{cb} \\ V_{td} & V_{ts} & V_{tb} \end{pmatrix} \tag{1}$$

The amplitude of the transition from a quark q_j to a quark q_i, through the weak interaction and the emission of a W ($q_j \to q_i W^-$) is proportional to the matrix element V_{ij}. The same transition between the anti-quarks ($\bar{q}_j \to \bar{q}_i W^+$) has an amplitude proportional to the complex conjugate of this matrix element, V_{ij}^*. Since there are 3 quark families, the CKM matrix is a 3×3 unitary matrix which can be parameterised by four numbers: three modules and one phase. Because of this phase which appears in decay amplitudes, CP violation can arise from quantum mechanics interference effects when summing several amplitudes with different phases.

The unitarity condition of the CKM matrix can be graphically represented with triangles in the complex plane which illustrate relations between the elements of the matrix. The most commonly used triangle is called the "Unitarity Triangle" and is shown in Fig. 2.

A large number of phenomena are explained by the CKM mechanism and depend only on the four free parameters of the matrix. Combining the different experimental measurements related to the CKM matrix provides a powerful test of the validity of the CKM formalism and of the Standard Model, verifying that all these measurements are consistent between them. The combination of the experimental data can be obtained with different methods, such as that presented in Ref. [6] or that presented in Ref. [7], which give similar results. Fig. 3 represents the result of the combination of existing

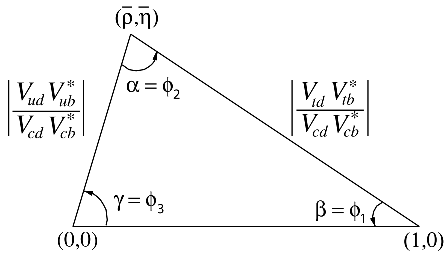

Fig. 2. Unitarity Triangle.

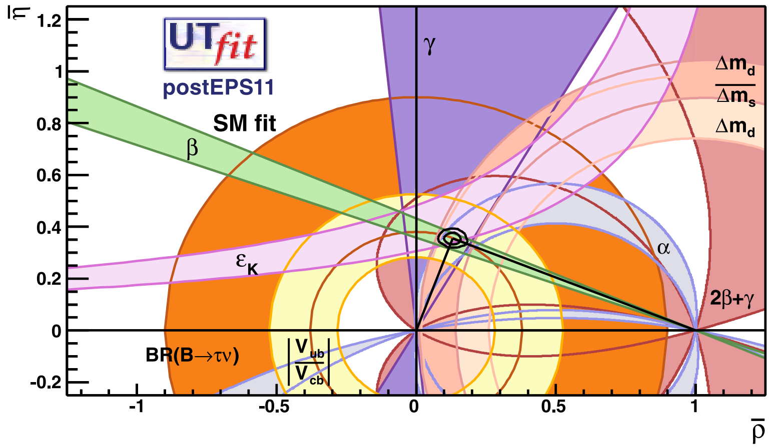

Fig. 3. Global fit of the Unitarity Triangle.

experimental data, obtained from Ref. [7]. On this figure, the fit to the different constraints is represented by the ellipses around the triangle apex, showing that all experimental measurements are compatible with the Standard Model description of the CP violation though the CKM matrix.

A large number of the precise experimental constraints used in Fig. 3 were obtained from analyses made at B-factories (e^+e^- colliders at a centre-of-mass energy of 10.6 GeV, BaBar [8] and BELLE [9]) during the last ten years, mainly using B^0 and B^+ meson decays, i.e. studying mesons formed by a b quark and a light quark (d or u).

3. Search for New Physics in CP violation

The CP violation is present in the Standard Model, but it is far too small to explain the matter–anti-matter asymmetry in the Universe. This suggests that there may be other CP violation mechanisms beyond the Standard Model and that studying CP violation could be an interesting probe of New Physics. Since recent experimental measurements confirmed the Standard Model description of CP violation with B^0 decays up to a precision of 10–20%, two main research paths will be explored by new experiments:

- Improve the precision of the measurements increasing the available statistics and using newer experimental techniques;
- Study decay modes not covered so far, such as the decays of the heavier B_s^0 meson, formed by a b and a s quark and which could not be produced at B factories, being too heavy.

The Large Hadron Collider (LHC) at CERN provides a good experimental environment for these studies because the production cross-section of B hadrons at the LHC is large and because the centre-of-mass energy is large enough to produce all types of B hadrons.

One potentially interesting measurement is to study CP violation in B_s^0 decays, that are abundantly produced at the LHC and which can be studied by the LHCb experiment. The B_s^0 meson is not an eigenstate of weak interactions and can oscillate between the B_s^0 state and the $\bar{B}_s^0$ state, through processes such as that represented by the Feynman diagram of Fig. 4.

The main characteristics of the B_s^0 meson are [10]:

- mass: $m = 5366.3 \pm 0.6$ MeV/c^2 [11];
- lifetime: $\tau = 1.425 \pm 0.041$ ps [12];
- oscillation frequency: $\Delta m_s = 2\pi f = 17.77 \pm 0.12$ ps^{-1} [13].

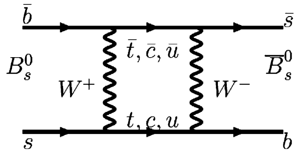

Fig. 4. Feynman diagram of one B_s^0–$\bar{B}_s^0$ oscillation process.

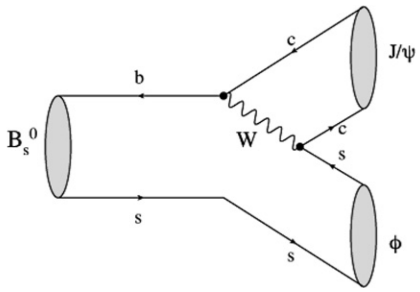

Fig. 5. Feynman diagram of the tree process of the $B_s^0 \to J/\psi\phi$ decay.

Table 1
Characteristics of the LHC accelerator, for the current running (left column) and the design values (right column).

	Current	Design
Proton collision energy	3.5 TeV	7 TeV
Magnet field of the bending magnet	4.16 T	8.33 TeV
Number of protons per bunch	1.15×10^{11}	1.15×10^{11}
Number of bunches in one ring	1380	2808
Space between bunches	50 ns	25 ns
Beam transverse size (at collision points)	31 μm	17 μm
Stored energy per ring	90 MJ	360 MJ

The golden decay mode to study CP violation in B_s^0 decays is the decay mode $B_s^0 \to J/\psi\phi$, where the J/ψ meson is observed in the decay mode $J/\psi \to \mu^+\mu^-$ and the ϕ meson in $\phi \to K^+K^-$. The Feynman diagram of this decay is shown in Fig. 5. The $J/\psi\phi$ final state is a state with two spin-1 particles, produced from a spin-0 particle, and is thus a combination of CP-odd and CP-even eigenstates. These two CP states are disentangled on a statistical basis with an angular analysis of the decay products. The final state can be reached from an initial B_s^0 state through two paths:

- direct decay: $B_s^0 \to J/\psi\phi$. The amplitude of this process has a weak phase equal to ϕ_D;
- or after having oscillated to a $\bar{B}_s^0$ state: $B_s^0 \to \bar{B}_s^0 \to J/\psi\phi$. The amplitude of this process has a weak phase equal to $\phi_M - \phi_D$, where ϕ_M is the weak phase of the mixing process.

The total amplitude of the decay $B_s^0 \to J/\psi\phi$ is the sum of the amplitudes of the two processes and the weak phase between the two amplitudes, equal to $\phi_s = \phi_M - 2\phi_D$ is the parameter to be measured by the analysis. ϕ_s is experimentally accessible through the time-dependent decay rate of B_s^0 initial states (i.e. B_s meson in the state B_s^0 at the time they are produced) and of $\bar{B}_s^0$ initial states (i.e. B_s meson in the state $\bar{B}_s^0$ at the time they are produced):

$$\frac{\mathrm{d}\Gamma(B_s^0 \to J/\psi\phi)}{\mathrm{d}t} = f(\phi_s) \quad \text{and} \quad \frac{\mathrm{d}\Gamma(\bar{B}_s^0 \to J/\psi\phi)}{\mathrm{d}t} = \bar{f}(\phi_s) \tag{2}$$

Within the Standard Model, the value of ϕ_s is almost equal to $\phi_s \simeq -2\arg\frac{V_{cs}V_{tb}^*}{V_{cs}V_{cb}^*}$, and V_{ij} are CKM matrix elements. The indirect determination of this phase in the Standard Model gives $\phi_s^{SM} = 0.0363^{+0.0016}_{-0.0015}$ rad [14].

One of the reasons why this decay mode is important to probe New Physics is that the B_s mixing occurs through a box diagram where heavy new particles could contribute and modify the mixing phase ϕ_M, and thus the measured value of ϕ_s would be different from ϕ_s^{SM}. The other reason is that previous measurements of ϕ_s in $B_s^0 \to J/\psi\phi$ decays made at the Tevatron accelerator by the CDF [15] and the D0 [16] Collaborations showed hints of a deviation from the Standard Model although these measurements had large statistical uncertainties of the order of 0.5 rad.

4. The LHCb experiment at the LHC

The Large Hadron Collider (LHC) [17] is a particle accelerator that collides protons (and also heavy ions). It is located at CERN (Geneva, Switzerland) in an underground tunnel of 27 km circumference. The first proton–proton collisions at a centre-of-mass energy of 3.5 TeV were obtained in 2010. Table 1 summarises the main characteristics of the accelerator. The design values will be reached after a one year stop in year 2013.

The LHC proton beams collide at four interaction points where four experiments are located: ALICE [18], ATLAS [19], CMS [20] and LHCb [21]. The LHCb experiment is located at the Interaction Point 8, close to the Geneva airport, in a 100 m deep underground cavern. The LHCb Collaboration is composed of 730 scientists from 15 different countries.

The key features of the LHCb detector are:

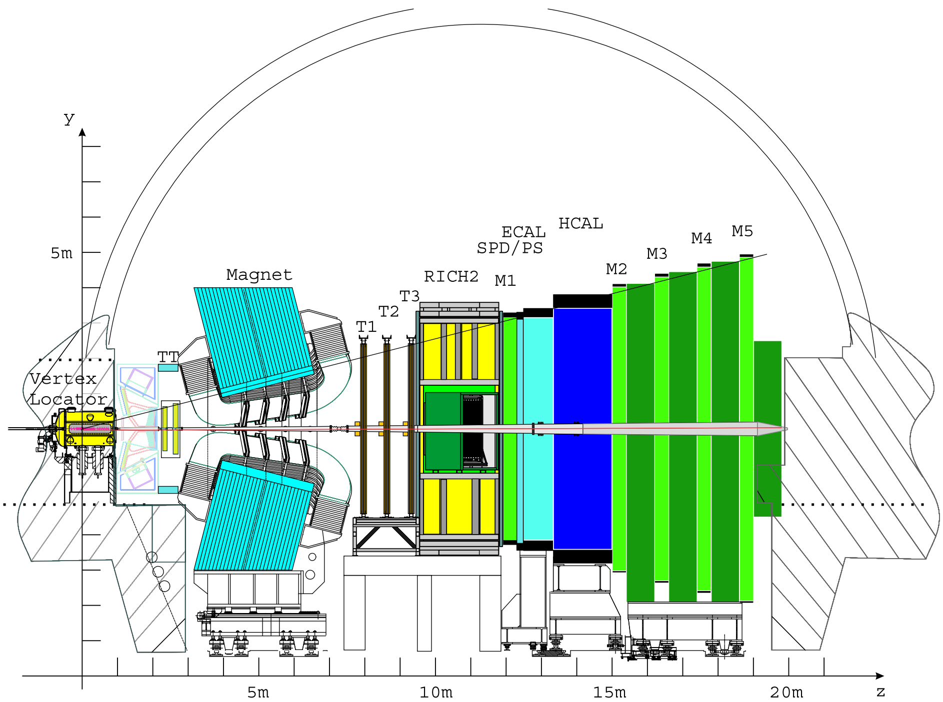

Fig. 6. Side view of the LHCb detector showing the Vertex Locator (VELO), the dipole magnet, the two RICH detectors, the four tracking stations TT and T1–T3, the Scintillating Pad Detector (SPD), Preshower (PRS), Electromagnetic (ECAL) and Hadronic (HCAL) calorimeters, and the five muon stations M1–M5.

- A versatile trigger scheme efficient for final states with leptons (electrons and muons) and charged hadrons, able to detect decay modes with small branching fractions;
- Excellent proper time resolution thanks to precise measurements of decay positions;
- Precise particle identification;
- Precise momentum reconstruction to reject efficiently background due to random combinations of particles.

A schematic layout of the detector is shown in Fig. 6. It consists of a vertex locator (VELO), a charged-particle tracking system with a large aperture dipole magnet, aerogel and gas Ring Imaging Cherenkov counters (RICH), electromagnetic (ECAL) and hadronic (HCAL) calorimeters and a muon system. A complete description of the detector characteristics can be found in Ref. [21]. The collision point of the LHC beams is located inside the VELO.

Two sub-detectors of the experiment are based on wire detectors and use detection techniques invented by Georges Charpak [22]. The Outer Tracker (located in the T1, T2 and T3 tracking stations shown in Fig. 6) is a drift-time detector with a mixture of Argon and CO_2 as counting gas and with a resolution on the track trajectory positions equal to 200 μm, allowing one to obtain the necessary track particle momentum resolution. The Muon Detector (stations M1–M5 in Fig. 6) includes Multi Wire Proportional Chambers using an Argon, CO_2 and CF_4 gas mixture. The Muon Detector allows to identify muons with high efficiency and is also participating to the triggering of the interesting events because it can detect muons in a processing time less than 25 ns.

The trigger system is also fundamental for the experiment. Out of the collisions which occur at a rate of 10 MHz, only a small fraction (2 kHz) contains events analysed by the experiment. The role of the trigger system is to detect early, at the time the collision occurs, interesting events and to reject the other ones. It is based on two levels:

- A first level which uses information from fast sub-detectors (calorimeters and muon detectors) to detect particles with high transverse momentum, which is an indication of the possible presence of a *b*-hadron in the event. This trigger level is realised in dedicated electronics boards and reduces the collision rate from 10 MHz to 1 MHz.
- A second level which uses information from all sub-detectors. This trigger level is realised in computer farms (10 000 CPU) and can thus be reprogrammed and be adjusted to follow the needs of the experiment. The event rate is reduced to 2 kHz after this stage and the events accepted by the trigger system are written on disk to be analysed in detail.

5. Measurement of ϕ_s at LHCb

The LHCb sub-detectors give information about the charged particle trajectories, bent by the dipole magnet, about the energy of neutral particles, and about the type of stable particles produced by LHC collisions. In order to measure ϕ_s as

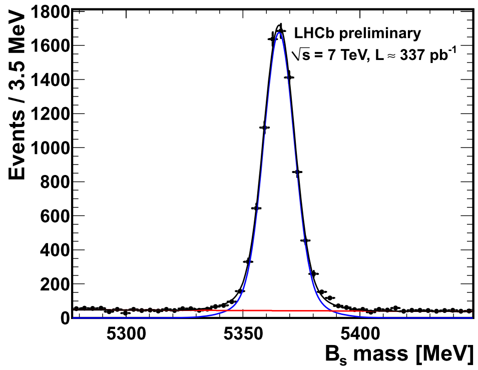

Fig. 7. Invariant mass of $B_s^0 \to J/\psi\phi$ candidates. (For interpretation of the references to color in this figure, the reader is referred to the web version of this article.)

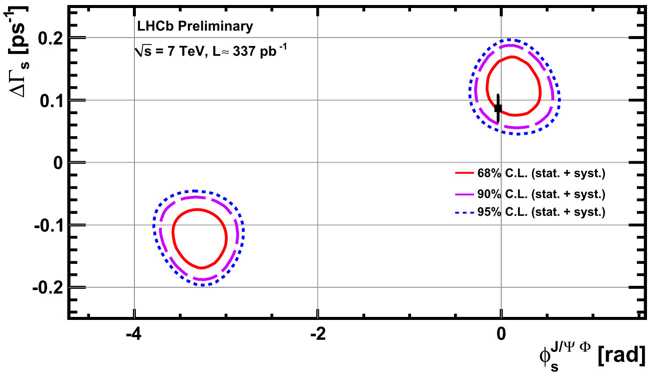

Fig. 8. Confidence level regions for ϕ_s. The theoretical predicted Standard Model value is shown with a black square.

described above, from the detector information one must:

- Detect B_s^0 and $\bar{B}_s^0$ decays to the $J/\psi(\to \mu^+\mu^-)\phi(\to K^+K^-)$ final state;
- Determine ("tag") if the initial state is a B_s^0 or a $\bar{B}_s^0$ state, since this cannot be determined from the final state only;
- Determine the proper time of the B_s^0 or $\bar{B}_s^0$ when it decays.

Very schematically, the measured time-dependent decay rate of $B_s^0 \to J/\psi\phi$ is proportional to

$$\sin(\phi_s) \times \sin(\Delta m_s t) \times (1 - 2\omega_{\text{tag}}) \tag{3}$$

where t is the proper time of the B_s^0 when it decays and ω_{tag} is the "mistag fraction", i.e. the probability to be wrong when "tagging" the initial state. At LHCb, the value of ω_{tag} is 36%. "Tagging" is done using the properties of events containing a B_s^0. In particular, an event with a b quark always contains a $\bar{b}$ quark. Identifying the type of the second b with its decay properties allows one to infer the type of the B_s^0 of interest. Eq. (3) indicates also that the reconstructed proper time precision must be better than the sine period of 350 fs. The LHCb detector achieved with the data collected in 2011 a time resolution of 50 fs, enough to perform the ϕ_s measurement.

The first measurement of ϕ_s at LHCb [23] was realised analysing the LHC collision data recorded up to July 2011. This corresponds to an integrated luminosity of 337 pb^{-1}. With these data, 8276 ± 94 signal $B_s^0 \to J/\psi\phi$ candidates were detected. The invariant mass distribution of these candidates is shown in Fig. 7, with a low background, indicated with a red line in the figure.

The value of ϕ_s is extracted from a fit to the time dependent decay rates of initial B_s^0 and $\bar{B}_s^0$ states, taking into account experimental resolutions and mistag. The obtained result for one of the two possible solutions is

$$\phi_s = 0.13 \pm 0.18\ (\text{stat.}) \pm 0.07\ (\text{syst.}) \tag{4}$$

where the first uncertainty is statistical and the second systematic. The other solution, due to symmetries in the decay rate, is farther away from the Standard Model prediction. Fig. 8 shows the likelihood confidence regions, compared to the Standard Model prediction for ϕ_s. No evidence of deviation from the Standard Model is observed. This is currently the most precise experimental measurement of ϕ_s. The precision of the measurement is dominated by statistical uncertainties. The

LHCb experiment is expected to collect 1 fb^{-1} of collision data until the end of year 2011, with which the analysis will be updated. The systematic uncertainty is dominated by the knowledge of the background and by the knowledge of the detection effects on the angular distribution of the decay products, used to separate the different CP state contributions. This knowledge will also improve in the near future, and a measurement with an error of the same order as the theoretical error could be obtained in the next years, allowing one to test precisely the Standard Model.

6. Conclusions

The first measurements related to CP violation from the LHCb Collaboration have been obtained during the Summer 2011. An illustrative example has been detailed here. It is representative of the set of results which do not show for the moment any failure of the Standard Model. Data accumulated during the next months will allow one to obtain more precise measurements of and to conclude on the presence of New Physics affecting CP violation in B_s^0 decays.

Other analyses are also conducted with the data recorded by the LHCb experiment. They concern measurements of CP violation in other B decay modes, such as the measurement of the γ angle of the Unitarity Triangle, or measurements of branching fractions of rare B and D decay modes, such as the decay $B_s^0 \to \mu^+\mu^-$. These analyses will also contribute to a precise determination of the Standard Model parameters related to CP violation, or could reveal the presence of New Physics.

References

[1] P.A.M. Dirac, Proc. R. Soc. Lond. A 117 (1928) 610.
[2] C. Anderson, Phys. Rev. 43 (1933) 491.
[3] A. Bindi, Nucl. Instrum. Methods A 617 (2010) 462.
[4] A.D. Sakharov, Pisma Zh. Eksp. Teor. Fiz. 5 (1967) 32.
[5] N. Cabibbo, Phys. Rev. Lett. 10 (1963) 531;
M. Kobayashi, T. Maskawa, Progr. Theoret. Phys. 49 (1973) 652.
[6] CKMfitter Group, J. Charles, et al., Eur. Phys. J. C 41 (2005) 1, hep-ph/0406184, updated results and plots available at http://ckmfitter.in2p3.fr.
[7] UTfit Collaboration, M. Bona, et al., JHEP 0507 (2005) 28, hep-ph/0501199.
[8] BaBar Collaboration, B. Aubert, et al., Nucl. Instrum. Methods Phys. Res. A 479 (2002) 1.
[9] BELLE Collaboration, A. Abashian, et al., Nucl. Instrum. Methods Phys. Res. A 479 (2002) 117.
[10] Particle Data Group, K. Nakamura, et al., J. Phys. G 37 (2010) 075021.
[11] CDF Collaboration, D. Acosta, et al., Phys. Rev. Lett. 96 (2006) 202001.
[12] D0 Collaboration, V.M. Abazov, et al., Phys. Rev. Lett. 97 (2006) 241801.
[13] CDF Collaboration, A. Abulencia, et al., Phys. Rev. Lett. 97 (2006) 242003.
[14] A. Lenz, et al., Phys. Rev. D 83 (2011) 036004, arXiv:1008.1593 [hep-ph].
[15] CDF Collaboration, Public note CDF/ANAL/BOTTOM/PUBLIC/10206, 2010.
[16] D0 Collaboration, D0 Conference note 6098-CONF, 2010.
[17] L. Evans, P. Bryant, et al., JINST 3 (2008) S08001.
[18] ALICE Collaboration, K. Aamodt, et al., JINST 3 (2008) S08002.
[19] ATLAS Collaboration, G. Aad, et al., JINST 3 (2008) S08003.
[20] CMS Collaboration, R. Adolphi, et al., JINST 3 (2008) S08004.
[21] LHCb Collaboration, A. Augusto Alves, et al., JINST 3 (2008) S08005.
[22] G. Charpak, R. Bouclier, T. Bressani, J. Favier, C. Zupancic, Nucl. Instrum. Methods 62 (1968) 262.
[23] LHCb Collaboration, LHCb-CONF-2011-049, 2011.